

1
2
3
4
5
6
7

Interference of Neuronal TrkB Signaling by the Cannabis-Derived Flavonoids Cannflavins A and B

Jennifer Holborn^{1*}, Alicya Walczyk-Mooradally^{1*}, Colby Perrin¹, Begüm Alural¹, Cara Aitchison¹, Adina Borenstein¹, Jibrán Y. Khokar², Tariq A. Akhtar¹, Jasmin Lalonde¹

¹ Department of Molecular and Cellular Biology, University of Guelph, 50 Stone Road E, Guelph, ON N1G 2W1, Canada.

² Department of Biomedical Science, University of Guelph, 50 Stone Road E, Guelph, ON N1G 2W1, Canada

* J.H. and A.W.M. contributed equally to this report.

8
9
10
11
12
13
14
15

Correspondence to: **Jasmin Lalonde**

Email: jlalon07@uoguelph.ca
Phone: (519) 824-4120 x. 54706
ORCID: 0000-0002-6797-1894

16 Keywords: Cannflavins; flavonoids; TrkB; BDNF; Arc

17 **ABSTRACT**

18 Cannflavins A and B are flavonoids that accumulate in the *Cannabis sativa* plant. These
19 specialized metabolites are uniquely prenylated and highly lipophilic, which, *a priori*, may permit
20 their interaction with membrane-bound enzymes and receptors. Although previous studies found
21 that cannflavins can produce anti-inflammatory responses by inhibiting the biosynthesis of pro-
22 inflammatory mediators, the full extent of their cellular influence remains to be understood. Here,
23 we studied these flavonoids in relation to the Tropomyosin receptor kinase B (TrkB), a receptor
24 tyrosine kinase that is activated by the growth factor brain-derived neurotrophic factor (BDNF).
25 Using mouse primary cortical neurons, we first collected evidence that cannflavins prevent the
26 accumulation of Activity-regulated cytoskeleton-associated (Arc, also known as Arg3.1) protein
27 upon TrkB stimulation by exogenous BDNF in these cells. Consistent with this effect, we also
28 observed a reduced activation of TrkB and downstream signaling effectors that mediate *Arc*
29 mRNA transcription when BDNF was co-applied with the cannflavins. Of note, we also performed
30 a high-throughput screen that demonstrated a lack of agonist action of cannflavins towards 320
31 different G protein-coupled receptors, a result that specifically limit the possibility of a TrkB
32 transinactivation scenario via G protein signaling to explain our results with dissociated neurons.
33 Finally, we used Neuro2a cells overexpressing TrkB to show that cannflavins can block the growth
34 of neurites and increased survival rate produced by the higher abundance of the receptor in this
35 model. Taken together, our study offers a new path to understand the reported effects of
36 cannflavins and other closely related compounds in different cellular contexts.

37 1. INTRODUCTION

38 Flavonoids are polyphenolic compounds found in various plant-derived foods and beverages.
39 These phytochemicals represent a large family of molecules that can be classified into six main
40 subclasses, based on their chemical structure: flavonols, flavanols (also known as flavan-3-ols or
41 catechins), flavanones, flavones, anthocyanins, and isoflavones (Panche et al., 2016). Interestingly,
42 evidence suggests that moderate habitual intake of flavonoids can lower the risk of cardiovascular
43 disease, cancer, as well as all-cause mortality (Bondonno et al., 2019). Another purported benefit
44 of these natural products is their positive influence on brain health and function, as several
45 members of the flavonoid family have been found to promote neuroprotection, reduce
46 neuroinflammation, and enhance cognition (Vauzour et al., 2008; Jaeger et al., 2018; Bakoyiannis
47 et al., 2018). More precisely, flavonoids appear to modulate signaling pathways that are central to
48 the control of neuronal survival and plasticity, such as the MAPK-CREB and PI3K-mTOR
49 cascades (Vauzour et al., 2008; Jaeger et al., 2018). However, this particular line of inquiry has
50 been little studied and therefore represents an opportunity to identify new bioactive compounds
51 with therapeutic qualities among this family of phytochemicals.

52 Apart from the psychoactive molecule Δ^9 -tetrahydrocannabinol (THC) and other related
53 cannabinoids with only mild or no psychotropic effect, like cannabidiol (CBD) and cannabigerol
54 (CBG), the *Cannabis sativa* (*C. sativa*) plant also produces hundreds of specialized metabolites
55 including at least twenty different flavonoid compounds (Flores-Sanchez et al., 2008). Among
56 those, the flavones cannflavin A and cannflavin B (Figure 1A) are considered to accumulate
57 uniquely in *C. sativa* cultivars. Seminal work by Barrett and colleagues performed more than 30
58 years ago helped identify these two flavonoids and characterize them as inhibitors of prostaglandin
59 E₂ production with the ability to produce anti-inflammatory effects that are approximately thirty

60 times more potent than acetylsalicylic acid, better known as aspirin (Barrett et al., 1985; 1986).
61 However, a broader understanding of cannflavins' influence on cell biology in health and disease
62 did not progress much since their initial description because of challenges associated with their
63 extraction and the various political landscapes that limited their distribution. Nevertheless, some
64 pre-clinical studies have provided intriguing new details about these molecules in recent years. For
65 instance, the unnatural isomer of cannflavin B named FBL-03G (also known as caflanone) was
66 found to increase apoptosis of pancreatic cancer cells *in vitro* while animal tests showed that the
67 same small molecule could limit progression of metastatic pancreatic cancer (Moreau et al., 2019).
68 Additionally, another study reported a possible neuroprotective effect of cannflavin A at
69 concentrations lower than 10 μM that was attributed to the ability of this molecule to reduce
70 aggregation of β amyloid through direct docking in the hydrophobic groove of the protein (Eggers
71 et al., 2019). While these different findings provide novel insights about the pharmacological
72 potential of cannflavins, the full range of molecular changes induced by cannflavins in cells
73 remains to be described. To address this gap in our understanding of cannflavin pharmacology, we
74 therefore focused on identifying novel mechanisms of action of these two related cannabis-derived
75 metabolites in neuronal cells.

76 Cannflavins A and B are prenylated and highly lipophilic small molecules (Barrett et al., 1985;
77 Choi et al., 2004), a characteristic that allows them to easily accumulate into cells where they can
78 then presumably interact with different membrane-bound enzymes and receptors. Previously, we
79 published a chemogenomic analysis that aimed at identifying small molecule modulators of
80 Activity-regulated cytoskeleton-associated protein (Arc), which is a key regulator of
81 neuroplasticity and cognitive functions (Bramham et al., 2010; Korb et al., 2011; Kedrov et al.,
82 2019). Our approach in that project exploited the ability of the growth factor brain-derived

83 neurotrophic factor (BDNF) to promote abundant *Arc* mRNA expression followed by nuclear
84 accumulation of the protein product in mouse primary cortical neurons via activation of
85 Tropomyosin receptor kinase B (TrkB) receptor (Lalonde et al., 2017). Here, we have adapted this
86 assay to test the two cannflavins and found evidence of TrkB signaling interference by both
87 molecules. These results then led us to complete a secondary high-throughput screen to test
88 possible agonist activity of these flavonoids on G protein-coupled receptors (GPCRs), as well as
89 other biochemical assays to confirm the influence of cannflavins and pinpoint their potential target
90 engagement. These specific efforts suggest a model where cannflavins interfere with TrkB activity
91 through direct inhibitory action on the receptor. Finally, image-based cellular test with
92 immortalized Neuro2a cells ectopically expressing TrkB allowed us to demonstrate the capacity
93 of cannflavins to block BDNF-induced neurite outgrowth. In summary, our study supports the
94 classification of cannflavins as candidate inhibitors of TrkB receptor signaling in neuronal cells.

95

96 **2. METHODS**

97 *2.1 Cell culture and transfection*

98 Developing cerebral cortex from E16.5 CD-1 mouse embryos were dissected and then dissociated
99 in trypsin solution for 15 min followed by three washes with phosphate-buffered saline (PBS).
100 Trypsinized tissue was gently triturated to produce single cell suspension. Next, cells were seeded
101 in poly-L-lysine/laminin coated 6-well plates at a density of 1.5×10^6 per well and maintained in
102 Neurobasal medium containing B27 supplement (2%, Invitrogen, Grand Island, NY), penicillin
103 (50 U/ml, Invitrogen), streptomycin (50 µg/ml, Invitrogen) and glutamine (1 mM, Sigma). For
104 experiments involving BDNF (PeproTech, Rocky Hill, NJ), the growth factor was added directly
105 to the culture medium at a final concentration of 100 ng/ml for the indicated period of time.

106 Preparation of mouse primary cortical neuron cultures was approved by the University of Guelph
107 Animal Care Committee and carried out according to institutional guidelines.

108 For neurite outgrowth assay, Neuro2a cells were cultured in DMEM [supplemented with 10%
109 HyClone FetalClone II serum (Cytiva, Global Life Sciences Solutions, Marlborough, MA),
110 penicillin (50 units/ml), and streptomycin (50 µg/ml)] and transfected overnight using
111 Lipofectamine 2000 (Invitrogen) according to the manufacturer's protocol.

112

113 *2.2 Antibodies, plasmid, and pharmacological compounds*

114 The anti-Arc rabbit polyclonal affinity purified antibody (#156 003) was purchased from Synaptic
115 Systems (Goettingen, Germany). The antibody recognizing p42 Mapk (Erk2, sc-1647) was from
116 Santa Cruz Biotechnology (Santa Cruz, CA). The antibodies recognizing phosphorylated
117 TrkA^{Tyr490}/TrkB^{Tyr516} (#4619), phosphorylated p44/42 Mapk (Erk1/2^{Thr202/Tyr204}, #4370), Akt
118 (#4691), phosphorylated Akt^{Thr308} (#2965), phosphorylated Akt^{Ser473} (#4060), mTor (#2983),
119 phosphorylated mTor^{Ser2448} (#2971), and phosphorylated rpS6^{Ser240/244} (#2215) were acquired from
120 Cell Signaling Technology (Beverly, MA). The antibody detecting TrkB (MAB397) was acquired
121 from R&D Systems (Minneapolis, MN), and the one specific for mouse phosphorylated TrkB^{Tyr705}
122 (ab229908) was from Abcam (Waltham, MA). The β-actin (A1978) and M2 FLAG (F1804)
123 antibodies were from Sigma-Aldrich (St-Louis, MO), while the Map2 (AB5543) antibody was
124 purchased from EMD Millipore Corps (Billerica, MA). Finally, cross-absorbed horseradish
125 peroxidase-conjugated secondary antibodies were from Invitrogen.

126 The pCMV6-Ntrk2-Myc-DDK (FLAG) plasmid (MR226130) was purchased from OriGene
127 Biotechnologies (Rockville, MD). ECGC, genistein, and daidzein were from Sigma-Aldrich.

128 ANA-12 (Figure 1B) was from Tocris Bioscience (Bristol, UK) and U0126 was from Biosciences
129 (Thermo Fisher).

130 The synthesis and purification of cannflavins A and B were produced using the method of Rea
131 and colleagues (2019). Briefly, *Cannabis sativa* L. prenyltransferase 3 (CsPT3) was recombinantly
132 expressed in *Saccharomyces cerevisiae* and the microsomal fraction containing CsPT3 was
133 collected for *in vitro* enzyme assays. Assays containing 200 μ M chrysoeriol, 400 μ M GPP or
134 DMAPP, 1 mg/mL of microsomal protein, and 10 mM MgCl₂ in 100 mM Tris-HCl buffer were
135 conducted at 37°C for 120 min and terminated with the addition of 20% formic acid. Cannflavin
136 products were extracted with three volumes of ethyl acetate, the organic layer was dried under N₂
137 gas and resuspended in methanol. The products were purified by high-performance liquid
138 chromatography (HPLC) on an Agilent 1260 Infinity system equipped with a Waters
139 SPHERISORB 5 μ m ODS2 column, and eluted with a 20 min linear gradient from 45% to 95%
140 methanol in water containing 0.1% formic acid. Product identities were confirmed via liquid
141 chromatography-mass spectrometry (LC-MS) according to published methods (Rea et al., 2019)
142 (Supplementary Figure 1). Cannflavins produced *in vitro* were dried under nitrogen gas and
143 resuspended in dimethyl sulfoxide (DMSO). The final products were confirmed via HPLC, as
144 described above, and quantified by absorption at 340 nm relative to authentic standards.

145

146 2.3 Western blotting

147 For western blot analyses, cells were collected by scraping in ice-cold radioimmunoprecipitation
148 assay (RIPA) buffer (50 mM tris-HCl [pH 8.0], 300 mM NaCl, 0.5% Igepal-630, 0.5%
149 deoxycholic acid, 0.1% SDS, 1 mM EDTA) supplemented with a cocktail of protease inhibitors
150 (Complete Protease Inhibitor without EDTA, Roche Applied Science, Indianapolis, IN) and

151 phosphatase inhibitors (Phosphatase Inhibitor Cocktail 3, Sigma-Aldrich). One volume of 2×
152 Laemmli buffer (100 mM tris-HCl [pH 6.8], 4% SDS, 0.15% bromophenol blue, 20% glycerol,
153 200 mM β -mercaptoethanol) was added and the extracts were boiled for 5 min. Samples were
154 adjusted to an equal concentration after protein concentrations were determined using the BCA
155 assay (Pierce, Thermo Fisher Scientific). Lysates were separated using SDS-PAGE
156 (polyacrylamide gel electrophoresis) and transferred to a nitrocellulose membrane. After transfer,
157 the membrane was blocked in TBST (tris-buffered saline and 0.1% Tween 20) supplemented with
158 5% nonfat powdered milk and probed with the indicated primary antibody at 4°C overnight. After
159 washing with TBST, the membrane was incubated with the appropriate secondary antibody and
160 visualized using enhanced chemiluminescence (ECL) reagents according to the manufacturer's
161 guidelines (Pierce, Thermo Fisher Scientific).

162 The following procedure was used to quantify western blot analyses. First, equal quantity of
163 protein lysate as determined by the BCA assay was analyzed by SDS-PAGE for each biological
164 replicate. Second, the exposure time of the film to the ECL chemiluminescence was the same for
165 each biological replicate. Third, all the exposed films were scanned on a HP Laser Jet Pro M377dw
166 scanner in grayscale at a resolution of 300 dpi. Fourth, the look-up table (LUT) of the scanned tiff
167 images was inverted and the intensity of each band was individually estimated using the selection
168 tool and the histogram function in Adobe Photoshop CC 2021 software. Finally, the intensity of
169 each band was divided by the intensity of its respective loading control (β -actin) to provide the
170 normalized value used for statistical analysis.

171

172

173

174 *2.4 Immunocytochemistry*

175 Indirect immunofluorescence detection of antigens was carried out using cortical neurons cultured
176 on poly-L-lysine/laminin coated coverslips in 24-well plates at a density of 0.1×10^6 per well.
177 After experimental treatment, cells were washed twice with phosphate-buffered saline (PBS) and
178 fixed for 30 min at room temperature with 4% paraformaldehyde in PBS. After fixation, cells were
179 washed twice with PBS, permeabilized with PBST (PBS and 0.25% Triton X-100) for 20 min,
180 blocked in blocking solution (5% goat non-immune serum in PBS) for another 30 min, and finally
181 incubated overnight at 4°C with the first primary antibody in blocking solution. The next day,
182 coverslips were extensively washed with PBS and incubated for 2 hours at room temperature in
183 the appropriate fluorophore-conjugated secondary antibody solution [Alexa Fluor 488-, Alexa
184 Fluor 594, or Alexa Fluor 647-conjugated secondary antibody (Molecular Probes, Invitrogen) in
185 blocking solution]. After washes with PBS, the coverslips were incubated again overnight in
186 primary antibody solution for the second antigen, and the procedure for conjugation of the
187 fluorophore-conjugated secondary antibody was repeated as above. Finally, cell nuclei were
188 counterstained with 4',6-diamidino-2-phenylindole (DAPI), and coverslips were mounted on glass
189 slides with ProLong Antifade reagent (Invitrogen).

190 Cells cultured on coverslips from three independent biological replicates were imaged with a
191 Nikon Eclipse Ti2-E inverted microscope equipped with a motorized stage, image stitching
192 capability, and a 60× objective (Nikon Instruments, Melville, NY). A total of 30 images per
193 condition were analyzed, three biological replicates were performed where ten images were
194 analyzed at random. All cells within the 60X field were included in the analysis. Image analysis
195 was performed with ImageJ and NIS Elements and the following procedure was used to quantify
196 nuclear Arc level in response to BDNF-TrkB signaling. First, original raw tiff files were opened

197 and the nucleus of all neurons in the image was located based on Map2 or NeuN immunostaining,
198 then average pixel intensity corresponding to Arc immunofluorescence was measured for a 30-
199 pixel spot positioned at the center of the nuclear compartment. Second, for each measure of Arc
200 nuclear immunofluorescence pixel intensity, a measure of background pixel intensity from the
201 same image channel was acquired and subsequently subtracted from the Arc nuclear
202 immunofluorescence pixel intensity value. Finally, Arc immunofluorescence signal from untreated
203 samples was used to establish an objective threshold (two standard deviations above the nuclear
204 Arc immunofluorescence signal averaged from a representative population of untreated neurons)
205 which allowed for comparison of nuclear Arc expression between different experimental
206 conditions.

207

208 *2.5 Real-time reverse transcriptase PCR*

209 After experimental treatment, total RNA was isolated from primary cortical neuron cultures using
210 the TRIzol method (Invitrogen). The concentration of total RNA was measured using a NanoDrop
211 ND-8000 spectrophotometer (Thermo Fisher Scientific) and first-strand complementary DNA
212 (cDNA) was synthesized using the iScript cDNA Synthesis Kit (Bio-Rad, Hercules, CA). Real-
213 time PCRs were performed using gene-specific primers and monitored by quantification of SYBR
214 Green I fluorescence using a Bio-Rad CFX96 Real-Time Detection System. Expression was
215 normalized against *Gapdh* expression. The relative quantification from three biological replicates
216 was calculated using the comparative cycle threshold ($\Delta\Delta C_T$) method.

217 Primers for real-time reverse transcription PCR experiments were: *Arc* primer pair one, 5'-
218 TAGCCAGTGACAGGACCCAG-3' (forward) and 5'-CAGCTCAAGTCCTAGTTGGCAAA-3' (reverse);
219 *Arc* primer pair two, 5'- CGCCAAACCCAATGTGATCCT-3' (forward) and 5'-

220 TTGGACACTTCGGTCAACAGA-3' (reverse); *Gapdh*, 5'-ATGACCACAGTCCATGCCATC-3' (forward)
221 and 5'-CCAGTGGATGCAGGGATGATGTTC-3' (reverse).

222

223 2.6 PRESTO-Tango GPCR assay

224 Parallel receptorome expression and screening via transcriptional output, with transcription
225 activation following arresting translocation (PRESTO-Tango) was used to assess cannflavin A and
226 cannflavin B potential to stimulate G protein-coupled receptors (GPCRs) according to published
227 methods (Kroeze et al., 2015). Overall, 320 distinct nonolfactory human GPCRs were tested.

228

229 2.7 Neurite outgrowth assessment

230 Neuro2A cells transfected with a pCMV6-Ntrk2-Myc-DDK (FLAG) construct were selected with
231 G-418 (Geneticin) to produce a stable cell line that constitutively expresses Myc-FLAG tagged-
232 TrkB. For neurite outgrowth assessment, cells were seeded on 15 mm glass coverslips in 12-well
233 plates at a density of 2.0×10^4 per well and allowed to attach overnight. Next day, cells were treated
234 with recombinant BDNF (1 nM) plus cannflavins (10 μ M), ANA-12 (10 μ M), or vehicle control
235 (DMSO). Phase contrast digital images were collected with a Nikon Eclipse Ti2-E inverted
236 microscope and a 20 \times objective 24 hours after start of treatment (five fields per dish, three wells
237 per condition). Image analysis was completed using ImageJ software using the following
238 procedure. First, any cells with a fragmented nucleus were excluded from the analysis, therefore
239 the total number of viable cells was counted per field. Second, for all identified viable cells the
240 total number of neurites and number of cells with neurites longer than 2 cell bodies in diameter
241 were counted per field.

242

243

244 *2.8 Alamar Blue assay*

245 Neuro2A cells stably expressing pCMV6-Ntrk2-Myc-DDK (FLAG) were seeded in 96-well plates
246 at a density of 1.0×10^4 and allowed to attach overnight. Next day, cells were treated with
247 recombinant BDNF (1 nM) plus cannflavins (10 μ M), ANA-12 (10 μ M), or vehicle control
248 (DMSO). Resazurin sodium salt (Sigma-Aldrich) was dissolved in Hank's balanced salt solution
249 (Gibco) to make a 0.5 mM working solution. After 21 hours of treatment, working solution was
250 diluted 1:10 into the 96-well plate and incubated at 37°C for 3 hours. Fluorescence was measured
251 with excitation/emission at 570/590 nm using a fluorescence microplate reader. All samples were
252 completed in triplicate, and a background control reading (media with working solution) was
253 subtracted from each value.

254

255 *2.9 Statistics*

256 Unless mentioned otherwise, all results represent the mean \pm SEM from at least three independent
257 experiments. ANOVA followed by Tukey's or Dunnett's post hoc test for multiple comparisons
258 were performed where indicated.

259

260 **3. RESULTS**

261 *3.1 Impact of cannflavins on BDNF-induced Arc expression in mouse primary cortical neurons*

262 Previously, we completed a chemogenomic screen with primary mouse cortical neurons that
263 identified a suite of compounds that acted as Arc expression modifiers (Lalonde et al., 2017). Part
264 of this group included five distinct flavonoids (Figure 1C)—namely (–)-epigallocatechin (ECGC),
265 baicalin (BAI), 7,8-dihydroxyflavone (7,8-DHF), daidzein, and genistein—which were found to
266 enhance nuclear Arc protein levels above the control measure when co-applied at a final

267 concentration of 16.7 μ M with recombinant BDNF for 6 h. Searching for a possible explanation
268 to this phenomenon, we were intrigued by several studies that had linked each of these five
269 flavonoids to either enhancement of *BDNF* and/or *TrkB* mRNA expression, or to the potentiation
270 of downstream TrkB-dependent signaling (Pan et al., 2012; Gundimeda et al., 2014; Ding et al.,
271 2018; Lu et al., 2019). Based on these observations, we hypothesized that cannflavin A and
272 cannflavin B could act in a similar fashion and promote Arc protein abundance when added to
273 cultured mouse cortical neurons that were stimulated with exogenous BDNF. Unexpectedly,
274 though, western blot analysis assessing BDNF-induced Arc expression in conjunction with
275 cannflavins with concentrations of the flavonoids ranging between 1 to 20 μ M revealed an opposite
276 effect. Specifically, we found that application of cannflavins to cell culture media prevented the
277 normal increase in Arc protein by BDNF in a dose-dependent manner where 10-20 μ M of
278 cannflavin A, and all tested concentrations (1-20 μ M) of cannflavin B, resulted in significantly
279 less Arc protein abundance than seen in the BDNF-alone control measure (Figure 2A). To further
280 support this result, we repeated the experiment using fluorescent immunocytochemistry and
281 quantified nuclear Arc changes, as we had done previously in our chemogenomic screen (Lalonde
282 et al., 2017). Of note, we also tested the flavonol ECGC, as well as the isoflavone daidzein and
283 genistein, since those molecules were found to produce the opposite effect of increasing BDNF-
284 induced nuclear Arc levels according to our previous screening results. As shown in Figure 2B
285 and Supplementary Figure 2, cells that were co-treated with BDNF and 10 μ M daidzein or
286 genistein presented a moderate increase in the percentage of nuclei with Arc expression above
287 threshold in comparison to the BDNF-alone control. Interestingly, though, the ECGC condition
288 was similar on average to the BDNF-alone condition suggesting that the final concentration of this
289 specific flavonoid must be greater than 10 μ M to have an impact of TrkB-induced nuclear Arc

290 level. Most importantly, and consistent with our western blot analysis above, cultures treated with
291 BDNF and 1-10 μ M cannflavins presented similar overall trends in the reduction of Arc-positive
292 neuronal abundance in comparison to the unstimulated control (Figure 2C). Together, these results
293 confirm the observed discrepancy between cannflavins and the other flavonoids found in our
294 earlier screen, which focused on BDNF-induced Arc expression modifiers.

295 Next, to ascertain whether the cannflavins' influence on TrkB signaling and Arc protein levels
296 was produced before or after gene transcription, we performed a quantitative polymerase chain
297 reaction (qPCR) experiment using two pairs of primers targeting different regions of the *Arc*
298 transcript. Here, comparison of *Arc* mRNA abundance between untreated, BDNF-alone control,
299 and BDNF with cannflavin A (10 μ M) or cannflavin B (10 μ M) samples clearly indicated that
300 cannflavins prevent induction of *Arc* mRNA expression (Figure 2D), therefore suggesting that the
301 effect of these compounds must occur somewhere between the activation of TrkB receptors by
302 BDNF and the activation of the transcriptional machinery involved in *Arc* expression.

303

304 *3.2 Evaluating agonist potential of cannflavins on Tango GPCR assay*

305 Considering the transactivation crosstalk between GPCRs and receptor tyrosine kinases, including
306 TrkB (Rajagopal et al., 2004; 2006; El Zein et al., 2007), and recent evidence for GPCR
307 modulation/self-association by flavonoids on the latter (Herrera-Hernández et al., 2017; Ortega et
308 al., 2019), we speculated that one mechanism by which cannflavins could interfere on *Arc* mRNA
309 expression in cortical neurons involves activation of a G protein signal that transinactivates the
310 function of molecular cascades downstream of TrkB receptors responsible for *Arc* expression. To
311 explore this scenario, we tested the effect of cannflavins on the GPCRome, *en masse*, using the
312 PRESTO-Tango assay—an unbiased high-throughput screening approach adapted to identify

313 agonist activity of agents towards the large family of GPCRs (Kroeze et al, 2015). Interestingly,
314 applying cannflavin A revealed no effect on any of the 320 different GPCRs tested while
315 cannflavin B was found to produce only weak increase (4.4 fold-change) of GPR150 activity from
316 baseline, a negligible effect in comparison to the positive control (51.3 fold-change, dopamine D₂
317 receptor stimulated by quinpirole) (Figure 3). Faced with these results, we then re-focused our
318 attention on the possibility that cannflavins act more directly on the TrkB receptor and/or its
319 downstream signaling components.

320

321 *3.3 Elucidating cannflavins effects on TrkB signaling*

322 BDNF binding to the extracellular domain of a TrkB receptor stimulates its dimerization and the
323 phosphorylation of various intracellular tyrosine residues which is followed by the recruitment of
324 pleckstrin homology (PH) and SH2 domain containing proteins—such as FRS2, Shc, SH2B, and
325 SH2B2—that regulate distinct concurrent signaling cascades (Qian et al., 1998; Meakin et al.,
326 1999). To explore whether cannflavins interfere with the activation of TrkB receptors by BDNF
327 in primary cortical neurons, we used a western blotting approach and probed lysates with two P-
328 Trk antibodies: one specific to mouse P-TrkA/B^{Y499/515}, which is associated with the recruitment
329 of Shc adaptor proteins, and another specific to mouse P-TrkB^{Y705} in the catalytic domain of the
330 receptor (Figure 4A). This approach revealed that, indeed, cannflavins can prevent BDNF from
331 effectively stimulating its target receptor (Figure 4B). To further support this result, we tested the
332 activation of signaling pathways that are likely regulated downstream of TrkB, including the Ras-
333 Raf-MEK-Mapk and the PI3K/Akt/mTor cascades (Huang et al., 2003; Kowiański et al., 2018)
334 (Figure 4A). Interestingly, our analyses revealed that both cannflavin A and cannflavin B sharply
335 reduced normal increase in P-Mapk, P-Akt, P-mTor, and P-rpS6 levels produced by BDNF (Figure

336 4C). The fact that there were those changes in these three molecular pathways, which to a great
337 extent occurs in parallel with limited cross-interaction (Kowiański et al., 2018), strongly suggest
338 that cannflavins must act at an early stage in TrkB signal activation.

339

340 *3.4 Functional characterization TrkB inhibition by cannflavins on BDNF-dependent neurite*
341 *outgrowth*

342 Our biochemical analyses with mouse primary cortical neurons suggest that cannflavins A and B
343 have inhibitory activity towards TrkB receptors. In order to establish if this effect is sufficient to
344 limit cellular processes under the control of BDNF signaling, we used neuroblastoma Neuro2a
345 cells stably expressing Ntrk2 (TrkB)-Myc-FLAG to complete a neurite outgrowth experiment
346 (Figure 5A). As shown in Figure 5B, Neuro2a cells have low TrkB expression with negligible
347 phosphorylation of the receptor under basal conditions, while cells stably expressing the receptor
348 display greater responsiveness to exogenous application of BDNF—which is clearly demonstrated
349 by higher level of P-TrkB. Further, pre-application of cannflavins (20 μ M) with BDNF to the
350 culture media for 6 h reduced BDNF-induced TrkB phosphorylation (Figure 5C). Interestingly, we
351 did not observe a decrease in P-Mapk levels with treatment of ANA-12 or cannflavins as was
352 observed in cortical neurons (Figure 4C), a distinction that we attribute to the fact that
353 overexpression of TrkB in Neuro2A produced maximal phosphorylation of the p42 subunit of
354 Mapk and no change in signal when BDNF was added to the Neuro2a cells (Figure 5B). Most
355 importantly, neurite assays completed with and without the application of ANA-12, cannflavin A,
356 and cannflavin B revealed that all three compounds produced a significant decrease in the total
357 number of neurites per field (Figure 5D and E) and number of cells with processes twice the length
358 of the cell (Figure 5F) when applied at a final concentration of 10 μ M to culture media. Cell

359 viability was then measured using Alamar Blue cell survival assay, which revealed no significant
360 difference between the BDNF control condition and the BDNF plus ANA-12 or cannflavins
361 (Figure 5G). Of note, our measures of total number and length of neurites for the ANA-12 and
362 cannflavins conditions in this experiment were comparable to the baseline values observed in wild-
363 type Neuro2a cells not overexpressing TrkB (Supplementary Figure 3). Altogether, our results
364 here strongly support that cannflavins act on TrkB receptors, preventing BDNF activation of
365 downstream signaling of the receptor.

366

367 **4. DISCUSSION**

368 This study provides evidence for an inhibitory effect of cannflavins A and B, two flavonoids from
369 *C. sativa*, on BDNF-induced Arc expression through disruption of TrkB receptor signaling. These
370 results contrast our previous observations that other flavonoids exhibit a potentiating effect
371 towards BDNF-induced Arc accumulation in mouse primary cortical neurons (Lalonde et al.,
372 2017). Strikingly, the addition of cannflavin A or cannflavin B to the culture medium of mouse
373 primary cortical neurons at a minimum concentration of 5 μ M consistently prevented the induction
374 of Arc mRNA expression, suggesting that these molecules act between BDNF-activation of TrkB
375 receptors and transcription of the Arc gene. Therefore, we subsequently investigated the impact of
376 cannflavins on the downstream pathways of TrkB using biochemical analyses and uncovered a
377 consistent decrease in the activation of the Ras-Raf-Mek-Mapk and the PI3K/Akt/mTor cascades.
378 In connection with these results, we demonstrated that cannflavins inhibited BDNF-induced
379 neurite outgrowth in neuroblastoma Neuro2a cells stably overexpressing TrkB. Taken together,
380 our study provides a new path to better understand the effects that have been reported in recent

381 years about cannflavins and other closely related compounds against certain cancer cell types
382 (Brunelli et al., 2009; Moreau et al., 2019).

383

384 *4.1 Structural determinants of cannflavins activity towards TrkB*

385 All flavonoids have a basic flavan nucleus with two aromatic rings (the A and the B rings)
386 interconnected by a three-carbon-atom heterocyclic ring (the C ring), as illustrated in Figure 1C
387 for the flavone 7,8-dihydroxyflavone (7,8-DHF, also known as tropoflavin). Interestingly, a
388 previous study focusing on 7,8-DHF, which is a compound reported to mimic the physiological
389 activity of BDNF and stimulate TrkB signaling *in vitro* and *in vivo* (Jang et al., 2010; Zeng et al.,
390 2012), helps speculate about what structural feature could provide TrkB antagonistic activity to
391 cannflavins. Specifically, previous comparison of different 7,8-DHF derivatives on TrkB
392 phosphorylation and downstream Akt signaling revealed that the presence of a 3'-hydroxy group
393 (or to a lesser extent a 2'-hydroxy group) on the B ring confers a TrkB stimulatory effect to a 7,8-
394 DHF derivative compound whereas addition of a 4'-hydroxy group, as shown in Figure 6A with 7,
395 8, 4'-trihydroxyflavone and Figure 6B with 3, 5, 7, 8, 3, 4'-hexahydroxyflavone, inversely mediates
396 inhibition of the receptor (Liu et al., 2010). Since cannflavins A and B are both hydroxylated at
397 the 4' position on the B ring (Figure 1A), similar to compounds found by Liu and colleagues (2010)
398 interfering with TrkB phosphorylation in rat primary cortical neurons (Figures 6A and 6B), we
399 thus suspect that this specific structural feature is key in mediating the TrkB antagonistic effect
400 observed in our study. In this context, it will be revealing whether cannflavin derivatives with
401 different patterns of hydroxylation on the B ring produce a different activity towards TrkB and
402 downstream cellular effects.

403 In addition to 4' hydroxylation of the B ring, prenylation is another structural element that we
404 must consider in relation to the difference we consistently observed between cannflavin A and
405 cannflavin B towards TrkB. As seen in Figure 1A, cannflavin B has only one isoprene unit while
406 cannflavin A has two, making the later an overall larger and more lipophilic molecule.
407 Consequently, we speculate that the smaller size of cannflavin B may facilitate access and/or create
408 a stronger binding affinity to TrkB in a cellular context, which could then explain why we have
409 been measuring a more potent inhibitory response of the receptor phosphorylation and blunting of
410 downstream signaling with this specific compound. Here, though, we acknowledge that one
411 limitation to our study is we do not demonstrate direct interaction of cannflavins A and B with
412 TrkB at this point. Nevertheless, two specific results from our study support to a certain degree the
413 idea that a direct functional interaction most likely occur between cannflavins and TrkB. First, our
414 interrogation of the GPCRome using the PRESTO-Tango assay showed that cannflavins do not
415 stimulate the activity of more than 300 GPCRs, which rules out the possibility that cannflavins are
416 disrupting TrkB function through a GPCR transinactivation event in our cellular experiments
417 (Rajagopal et al., 2004; 2006; El Zein et al., 2007). And second, our experiment with Neuro2a
418 cells stably expressing TrkB reveals that cannflavins block the growth of neurites, as well as the
419 observed cell survival stimulatory effect, produced by exogenous BDNF application in this model.
420 Since these phenotypes are directly tied to the overexpression of TrkB, and that application of
421 cannflavins consistently returns neurite and survival measures to those of wild-type Neuro2a cells
422 (Supplementary Figure 3), we consider these results as evidence for a direct interaction between
423 cannflavins and TrkB. To conclude on this point, whether the activity of receptor tyrosine kinases
424 other than TrkB is interfered by cannflavins remains unknown and should be considered in future
425 research.

426 *4.2 Therapeutic potential of cannflavins*

427 Although cannflavins are recognized to produce potent anti-inflammatory effects by inhibiting the
428 biosynthesis of various pro-inflammatory mediators, including microsomal prostaglandin E₂
429 synthase-1 (mPGES-1) and 5-lipoxygenase (5-LO) (Barrett et al., 1985; 1986; Werz et al., 2014),
430 our study cautions that these flavonoids may not be adequate to intervene against
431 neuroinflammation or provide pro-cognitive effects because of their impact on TrkB signaling
432 (Jaeger et al., 2018). Also, recent evidence suggests that the therapeutic action on mood of both
433 typical and fast-acting antidepressants may be linked by their ability to directly bind TrkB
434 receptors and allosterically increase BDNF signaling (Casarotto et al., 2021). Based on that
435 specific information, and our results in this study, we consequently suspect that cannflavins may
436 exacerbate depressive mood. Keeping those important details in mind, we nevertheless believe that
437 cannflavin A and/or cannflavin B should be further studied in relation to clinical circumstances
438 where overactive or dysregulated TrkB signaling is a contributing factor. For instance, increased
439 TrkB expression was detected in low-grade astrocytoma and glioblastoma (Wadhwa et al., 2003;
440 Assimakopoulou et al., 2007), while BDNF-induced activation of TrkB has been found to increase
441 the viability of brain-tumor stem cells isolated from glioblastoma (Lawn et al., 2015). Furthermore,
442 a study uncovered a link between the ability of glioblastoma to make less invasive cancer cells
443 around them more aggressive via the transfer of TrkB-containing exosomes, revealing this way a
444 mechanism by which these tumours can influence their environment to promote disease
445 aggressiveness (Pinet et al., 2016), and other reports have shown that inhibition of TrkB-associated
446 signaling may be an effective strategy to limit the formation of astrocytomas (Ni et al., 2017) as
447 well as the survival of glioblastoma cancer cells (Pinheiro et al., 2017). Finally, accumulating
448 evidence support that TrkB signaling could also be a therapeutic target for other cancer types,

449 including lung (Sinkevicius et al., 2014; Chen et al., 2016), breast (Choy et al., 2017; Contreras-
450 Zárate et al., 2019), and pancreatic cancer (Oyama et al., 2021). Taken together, these studies
451 suggest that targeting TrkB signaling with cannflavins could provide therapeutic benefits against
452 different cancer types, in particular those affecting the nervous system.

453 Lastly, peripheral increase in BDNF appears to be common in autism spectrum disorder based
454 on meta-analysis evidence (Zheng et al., 2016), and the BDNF/TrkB pathway has been linked to
455 hyperexcitability caused by axonal transection and some forms of epileptogenesis (Lin et al.,
456 2020). Whether cannflavins could be valuable agents in those contexts should be tested. In
457 conclusion, our study expands the range of cellular effect for cannflavins beyond inflammation
458 and supports the examination in more detail of these compounds to attack brain cancer cells as
459 well as mitigate aberrant neurodevelopmental and circuit phenotypes that could be resulting from
460 uncontrolled BDNF-TrkB signaling.

461 **DATA AVAILABILITY STATEMENT**

462 The raw data supporting the conclusions of this article will be made available by the authors,
463 without undue reservation.

464

465 **ETHICS STATEMENT**

466 The use of mice for primary neuron cultures was reviewed and approved by the University of
467 Guelph Animal Care Committee.

468

469 **AUTHOR DISCLOSURE STATEMENT**

470 T.A.A. received sponsored research funding from Atlas 365 that was used for the preparation of
471 cannflavins used in this research. The other authors declare no conflict of interest.

472

473 **AUTHOR CONTRIBUTIONS**

474 J.H., A.W.M., B.A., J.Y.K., and J.L. planned and designed the experiments. C.P., J.Y.K., and
475 T.A.A. provided key resources, and J.H., A.W.M., B.A., and C.A. performed the research. J.H.,
476 A.W.M., B.A., C.P., C.A., and J.L. analyzed the data and prepared figures. J.H., A.W.M., and J.L.
477 wrote the manuscript with revisions from all other authors.

478

479 **ACKNOWLEDGMENTS**

480 We wish to thank Drs. Dyanne Brewer and Armen Charchoglyan for their assistance with mass
481 spectrometry analysis of cannflavins, as well as the NIMH Psychoactive Drug
482 Screening Program (NIMH-PDSP) for help collecting the Tango GPCR assay results presented in
483 this study. This work was supported by a Natural Sciences and Engineering Research Council of

484 Canada (NSERC) Discovery Grant (401389), the Canadian Foundation for Innovation (CFI,
485 037755), and generous start-up funding from the University of Guelph (all to J.L.). A.W.M was
486 supported by the University of Guelph (Graduate Tuition Scholarship).

487

488 **LIST OF ABBREVIATIONS**

489	Arc	activity-regulated cytoskeleton-associated
490	BDNF	brain-derived neurotrophic factor
491	CREB	cAMP-response element binding protein
492	GPCR	G protein-coupled receptors
493	Mapk	mitogen-activated protein kinase
494	mTOR	mammalian target of rapamycin
495	PI3K	phosphatidylinositol-3 kinase
496	THC	Δ^9 -tetrahydrocannabinol
497	TrkB	tropomyosin receptor kinase B

498 **REFERENCES**

- 499 Assimakopoulou, M., Kondyli, M., Gatzounis, G., Maraziotis, T., Varakis, J. (2007) Neurotrophin
500 receptors expression and JNK pathway activation in human astrocytomas. *BMC Cancer* 7,202.
- 501 Bakoyiannis, I., Daskalopoulou, A., Pergialiotis, V., Perrea, D. (2018) Phytochemicals and
502 cognitive health: Are flavonoids doing the trick? *Biomed. Pharmacother.* 190, 1488-1497.
- 503 Barrett, M.L., Gordon, D., Evans, F.J. (1985) Isolation from *Cannabis sativa* L. of cannflavin—a
504 novel inhibitor of prostaglandin production. *Biochem. Pharmacol.* 34, 2019-2024.
- 505 Barrett, M.L., Scutt, A.M., Evans, F.J. (1986) Cannflavin A and B, prenylated flavones from
506 *Cannabis sativa* L. *Experientia* 42, 452-453.
- 507 Bondonno, N.P., Dalgaard, F., Kyrø, C., Murray, K., Bondonno, C.P., Lewis, J.R., Croft, K.D.,
508 Gislason, G., Scalbert, A., Cassidy, A., Tjønneland, A., Overvad, K., Hodgson, J.M. (2019)
509 Flavonoid intake is associated with lower mortality in the Danish Diet Cancer and Health
510 Cohort. *Nat. Commun.* 10, 3651.
- 511 Bramham, C.R., Alme, M.N., Bittins, M., Kuipers, S.D., Nair, R.R., Pai, B., Panja, D., Schubert,
512 M., Soule, J., Tiron, A., Wibrand, K. (2010) The Arc of synaptic memory. *Exp. Brain Res.*
513 200, 125-140.
- 514 Brunelli, E., Pinton, G., Bellini, P., Minassi, A., Appendino, G., Moro, L. (2009) Flavonoid-
515 induced autophagy in hormone sensitive breast cancer cells. *Fitoterapia* 80, 327-332.
- 516 Casarotto, P.C., Girysh M., Fred S.M., Kovaleva, V., Moliner, R., Enkavi, G., Biojone, C.,
517 Cannarozzo, C., Priyadrashini Sahu, M., Kaurinkoski, K., Brunello, C.A., Steinzeig, A.,
518 Winkel, F., Patil, S., Vestring, S., Serchov, T., Diniz, C.R.A.F., Laukkanen, L., Cardon, I.,
519 Antila, H., Rog, T., Petteri Piepponen, T., Bramham, C.R., Normann, C., Lauri, S.E., Saarma,

- 520 M., Vattulainen, I., Castrén, E. (2021) Antidepressant drugs act by directly binding to TRKB
521 neurotrophin receptors. *Cell* 184, 1299-1313.
- 522 Cazorla, M., Prémont, J., Mann, A., Girard, N., Kellendonk, C., Rognan, D. (2011) Identification
523 of a low-molecular weight TrkB antagonist with anxiolytic and antidepressant activity in
524 mice. *J Clin Invest.* 121, 1846-1857.
- 525 Chen, B., Liang, Y., He, Z., An, Y., Zhao, W., Wu, J. (2016) Autocrine activity of BDNF induced
526 by the STAT3 signaling pathway causes prolonged TrkB activation and promotes human non-
527 small-cell lung cancer proliferation. *Sci. Rep.* 6, 30404.
- 528 Choi, Y.H., Hazekamp, A., Peltenburg-Looman, A.M., Frédérick, M., Erkelens, C., Lefeber, A.W.,
529 Verpoorte, R. (2004) NMR assignment of the major cannabinoids and cannabiflavonoids
530 isolated from flowers of *Cannabis sativa*. *Phytochem. Anal.* 15, 345-354.
- 531 Choy, C., Ansari, K.I., Neman, J., Hsu, S., Duenas, M.J., Li, H., Vaidehi, N., Jandial, R. (2017)
532 Cooperation of neurotrophin receptor TrkB and Her2 in breast cancer cells facilitates brain
533 metastases. *Breast Cancer Res.* 19, 51.
- 534 Contreras-Zárate, M.J., Day, N.L., Ormond, D.R., Borges, V.F., Tobet, S., Gril, B., Steeg, P.S.,
535 Cittelly, D.M. (2019) Estradiol induces BDNF/TrkB signaling in triple-negative breast cancer
536 to promote brain metastases. *Oncogene* 38, 4685-4699.
- 537 Ding, S., Zhuge, W., Hu, J., Yang, J., Wang, X., Wen, F., Wang, C., Zhuge, Q. (2018) Baicalin
538 reverses the impairment of synaptogenesis induced by dopamine burden via the stimulation
539 of GABA_AR-TrkB interaction in minimal hepatic encephalopathy. *Psychopharmacology* 235,
540 1163-1178.
- 541 Eggers, C., Fujitani, M., Kato, R., Smid, S. (2019) Novel cannabis flavonoid, cannflavin A
542 displays both a hormetic and neuroprotective profile against amyloid β -mediated

- 543 neurotoxicity in PC12 cells: Comparison with geranylated flavonoids, mimulone and
544 diplacone. *Biochem. Pharmacol.* 169, 113609.
- 545 El Zein N., Badran, B.M., Sariban, E. (2007) The neuropeptide pituitary adenylate cyclase
546 activating protein stimulates human monocytes by transactivation of the Trk/NGF pathway.
547 (2007) *Cell. Signal.* 19, 152-162.
- 548 Flores-Sanchez, I.J., Verpoorte, R. (2008) Secondary metabolism in Cannabis. *Phytochem. Rev.*
549 7, 615-639.
- 550 Gundimeda, U., McNeill, T.H., Fan, T.K., Deng, R., Rayudu, D., Chen, Z., Cadenas, E.,
551 Gopalakrishna, R. (2014) Green tea catechins potentiate the neuritogenic action of brain-
552 derived neurotrophic factor: role of 67-kDa laminin receptor and hydrogen peroxide.
553 *Biochem. Biophys. Res. Commun.* 445, 218-224.
- 554 Gupta, V.K., You, Y., Gupta, V.B., Klistorner, A., Graham, S.L. (2013) TrkB receptor signalling:
555 implications in neurodegenerative, psychiatric and proliferative disorders. *Int. J. Mol. Sci.* 14,
556 10122-10142.
- 557 Herrera-Hernández, M.G., Ramon, E., Lupala, C.S., Tena-Campos, M., Pérez, J.J., Garriga, P.
558 (2017) Flavonoid allosteric modulation of mutated visual rhodopsin associated with retinitis
559 pigmentosa. *Sci. Rep.* 7, 11167.
- 560 Huang, E.J., Reichardt, L.F. (2003) Trk receptors: Roles in neuronal signal transduction. *Annu.*
561 *Rev. Biochem.* 72, 609-642.
- 562 Jaeger, B.N., Parylak, S.L., Gage, F.H. (2018) Mechanisms of dietary flavonoid action in neuronal
563 function and neuroinflammation. *Mol. Aspects Med.* 61, 50-62.
- 564 Kedrov, A.V., Durymanov, M., Anokhin, K.V. (2019) The Arc gene: Retroviral heritage in
565 cognitive functions. *Neurosci. Biobehav. Rev.* 99, 275-281.

- 566 Korb, E., Finkbeiner, S. (2011) Arc in synaptic plasticity: from gene to behavior. *Trends Neurosci.*
567 34, 591-598.
- 568 Kowiański, P., Lietzau, G., Czuba, E., Waśkow, M., Steliga, A., Moryś, J. (2018) BDNF: A key
569 factor with multipotent impact on brain signaling and synaptic plasticity. *Cell. Mol.*
570 *Neurobiol.* 38, 579-593.
- 571 Kroeze, W.K., Sassano, M.F., Huang, X.P., Lansu, K., McCorvy, J.D., Giguère, P.M., Sciaky, N.,
572 Roth, B.L. (2015) PRESTO-Tango as an open-source resource for interrogation of the
573 druggable human GPCRome. *Nat. Struct. Mol. Biol.* 22, 362-369.
- 574 Lalonde, J., Reis, S.A., Sivakumaran, S., Holland, C.S., Wesseling, H., Sauld, J.F., Alural, B.,
575 Zhao, W.N., Steen, J.A., Haggarty, S.J. (2017) Chemogenomic analysis reveals key role for
576 lysine acetylation in regulating Arc stability. *Nat. Commun.* 8, 1659.
- 577 Lawn, S., Krishna, N., Pisklakova, A., Qu, X., Fenstermacher, D.A., Fournier, M., Vrionis, F.D.,
578 Tran, N., Chan, J.A., Kenchappa, R.S., Forsyth, P.A. (2015) Neurotrophin signaling via TrkB
579 and TrkC receptors promotes the growth of brain tumor-initiating cells. *J. Biol. Chem.* 290,
580 3814-3824.
- 581 Lin, T.W., Harward, S.C., Zhong Huang, Y., McNamara, J.O. (2020) Targeting BDNF/TrkB
582 pathways for preventing or suppressing epilepsy. *Neuropharmacology* 167, 107734.
- 583 Liu, X., Obianyo, O., Bun Chan, C., Huang J., Xue, S., Yang, J.J., Zeng, F., Goodman, M., Ye, K.
584 (2014) Biochemical and biophysical investigation of the brain-derived neurotrophic factor
585 mimetic 7,8-dihydroxyflavone in the binding and activation of the TrkB receptor. *J. Biol.*
586 *Chem.* 289, 27571-27584.
- 587

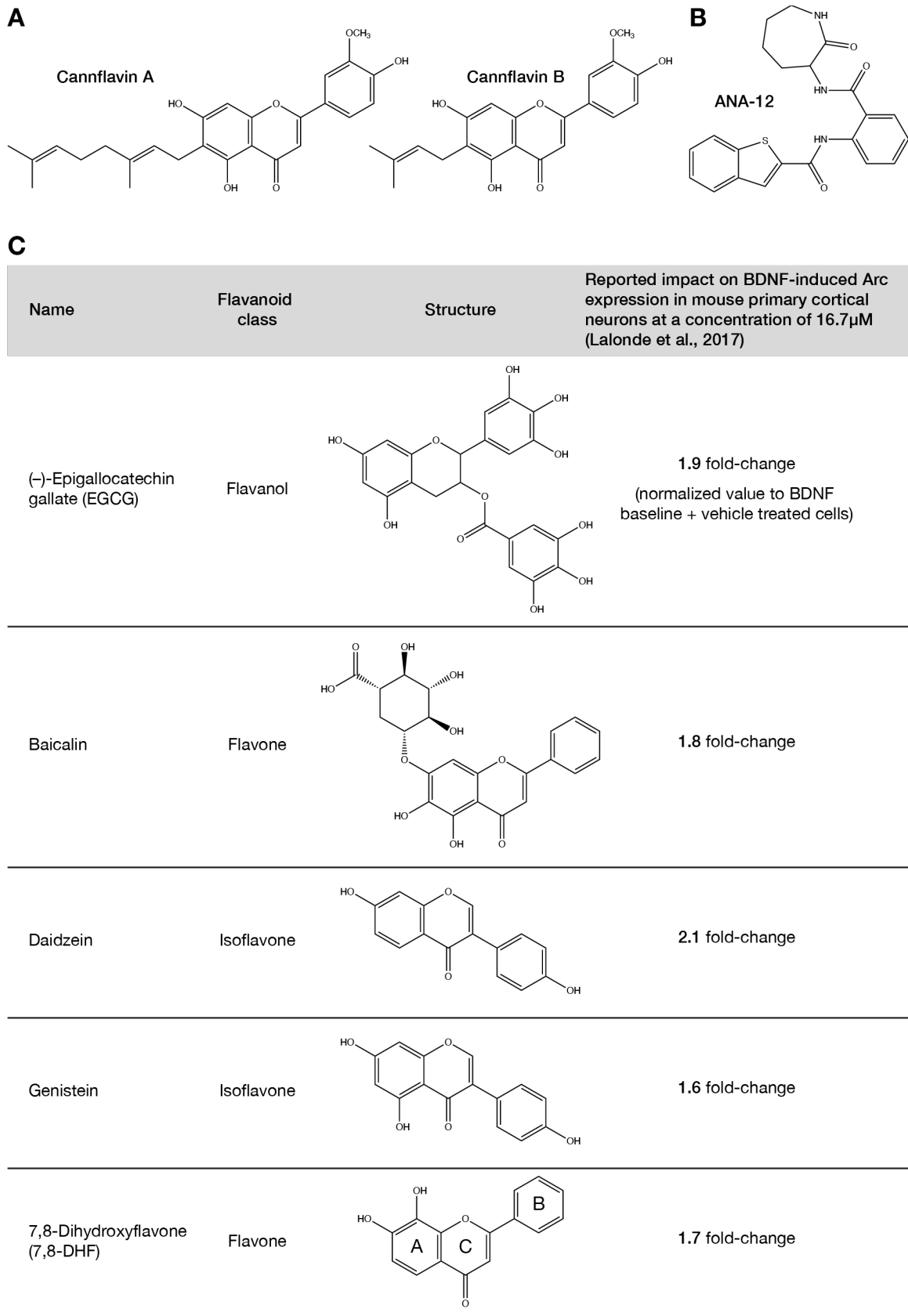
- 588 Lu, Y., Sun, G., Yang, F., Guan, Z., Zhang, Z., Zhao, J., Liu, Y., Chu, L., Pei, L. (2019) Baicalin
589 regulates depression behavior in mice exposed to chronic mild stress via the Rac/LIMK/cofilin
590 pathway. *Biomed. Pharmacother.* 116, 109054.
- 591 Meakin, S.O., MacDonald, J.I.S., Gryz, E.A., Kubum C.J., Verdim J.M. (1999) The signaling
592 adapter FRS-2 competes with Shc for binding to the nerve growth factor receptor TrkA. *J Biol*
593 *Chem.* 274, 9861-9870.
- 594 Moreau, M., Ibeh, U., Decosmo, K., Bih, N., Yasmin-Karim, S., Toyang, N., Lowe, H., Ngwa, W.
595 (2019) Flavonoid derivative of Cannabis demonstrates therapeutic potential in preclinical
596 models of metastatic pancreatic cancer. *Front. Oncol.* 9, 660.
- 597 Ni, J., Xie, S., Ramkissoon, S.H., Luu, V., Sun, Y., Bandopadhyay, P., Beroukhim, R., Robers,
598 T.M. Stiles, C.D., Segal, R.A., Ligon, K.L., Hahn, W.C., Zhao, J.J. (2017) Tyrosine receptor
599 kinase B is a drug target in astrocytomas. *Neuro Oncol.* 19, 22-30.
- 600 Oyama, Y., Nagao, S., Na, L., Yanai, K., Umebayashi, M., Nakamura, K., Nagai, S., Fujimura,
601 A., Yamasaki, A., Nakayama, K., Morisaki, T., Onishi, H. (2021) TrkB/BDNF signaling could
602 be a new therapeutic target for pancreatic cancer. *Anticancer Res.* 41, 4047-4052.
- 603 Ortega, J.T., Parmar, T., Jastrzebska, B. (2019) Flavonoids enhance rod opsin stability, folding,
604 and self-association by directly binding to ligand-free opsin and modulating its conformation.
605 *J. Biol. Chem.* 294, 8101-8122.
- 606 Pan, M., Han, H., Zhong, C., Geng, Q. (2012) Effects of genistein and daidzein on hippocampus
607 neuronal cell proliferation and BDNF expression in H19-7 neural cell line. *J. Nutr. Health*
608 *Aging* 16, 389-394.
- 609 Panche, A.N., Diwan, A.D., Chandra, S.R. (2016) Flavonoids: an overview. *J. Nutr. Sci.* 5, e47.

- 610 Pinet, S., Bessette, B., Vedrenne, N., Lacroix, A., Richard, L., Jauberteau, M.O., Battu, S., Lalloué,
611 F. (2016) TrkB-containing exosomes promote the transfer of glioblastoma aggressiveness to
612 YKL-40-inactivated glioblastoma cells. *Oncotarget* 7,50349-50364
- 613 Pinheiro, K.V., Alves, C., Buendia, M., Gil, M.S., Thomaz, A., Schwartzmann, G., de Farias, C.B.,
614 Roesler, R., Bowman, R.L., Wang, Q., Carro, A., Verhaak, R.G., Squatrito, M. (2017)
615 Targeting tyrosine receptor kinase B in gliomas. *Neuro Oncol.* 19,138-139.
- 616 Qian, X., Riccio, A., Zhang, Y., Ginty, D.D. (1998) Identification and characterization of novel
617 substrates of Trk receptors in developing neurons. *Neuron.* 21, 1017–1029.
- 618 Rajagopal, R., Chao, M.V. (2006) A role for Fyn in Trk receptor transactivation by G-protein-
619 coupled receptor signaling. *Mol. Cell Neurosci.* 33, 36-46.
- 620 Rajagopal, R., Chen, Z.Y., Lee, F.S., Chao, M.V. (2004) Transactivation of Trk neurotrophin
621 receptors by G-protein-coupled receptor ligands occurs on intracellular membranes. *J.*
622 *Neurosci.* 24, 6650-6658.
- 623 Rea, K.A., Cararetto, J.A., Al-Abdul-Wahid, M.S., Sukumaran A., Geddes-McAlister J., Rothstein
624 S.J., Akhtar T.A. (2019) Biosynthesis of cannflavins A and B from *Cannabis sativa* L.
625 *Phytochemistry*, 164, 162-171.
- 626 Sinkevicius, K.W., Kriegel, C., Bellaria, K.J., Lee, J., Lau, A.N., Leeman, K.T., Zhou, P., Beede,
627 A.M., Fillmore, C.M., Caswell, D., Barrios, J., Wong, K.K., Sholl, L.M., Schlaeger, T.M.,
628 Bronson, R.T., Chirieac, L.R., Winslow, M.M., Gaihis, M.C., Kim, C.F. (2014)
629 Neurotrophin receptor TrkB promotes lung adenocarcinoma metastasis. *Proc. Natl. Acad. Sci.*
630 *U.S.A.* 111, 10299-10304.
- 631 Vauzour, D., Vafeiadou, K., Rodriguez-Mateos, A., Rendeiro, C., Spencer, J.P. (2008) The
632 neuroprotective potential of flavonoids: a multiplicity of effects. *Genes Nutri.* 3, 115-226.

- 633 Wadhwa, S., Nag. T.C., Jindal, A., Kushwaha, R., Mahapatra, A.K., Sarkar, C. (2003) Expression
634 of the neurotrophin receptors Trk A and Trk B in adult human astrocytoma and glioblastoma.
635 J. Biosci. 28, 181-188.
- 636 Werz, O., Seegers, J., Schaible, A. M., Weinigel, C., Barz, D., Koeberle, A., Allegrone, G.,
637 Pollastro, F., Zampieri, L., Grassi, G., Appendino, G. (2014). Cannflavins from hemp sprouts,
638 a novel cannabinoid-free hemp food product, target microsomal prostaglandin E₂ synthase-1
639 and 5-lipoxygenase. *Pharmanutr.* 2, 53-60.
- 640 Zheng, Z., Zhang, L., Zhu, T., Huang, J., Mu, D. (2016) Peripheral brain-derived neurotrophic
641 factor in autism spectrum disorder: a systematic review and meta-analysis. *Sci. Rep.* 6, 31241.

FIGURE 1

HOLBORN, WALCZYK-MOORADALLY ET AL.



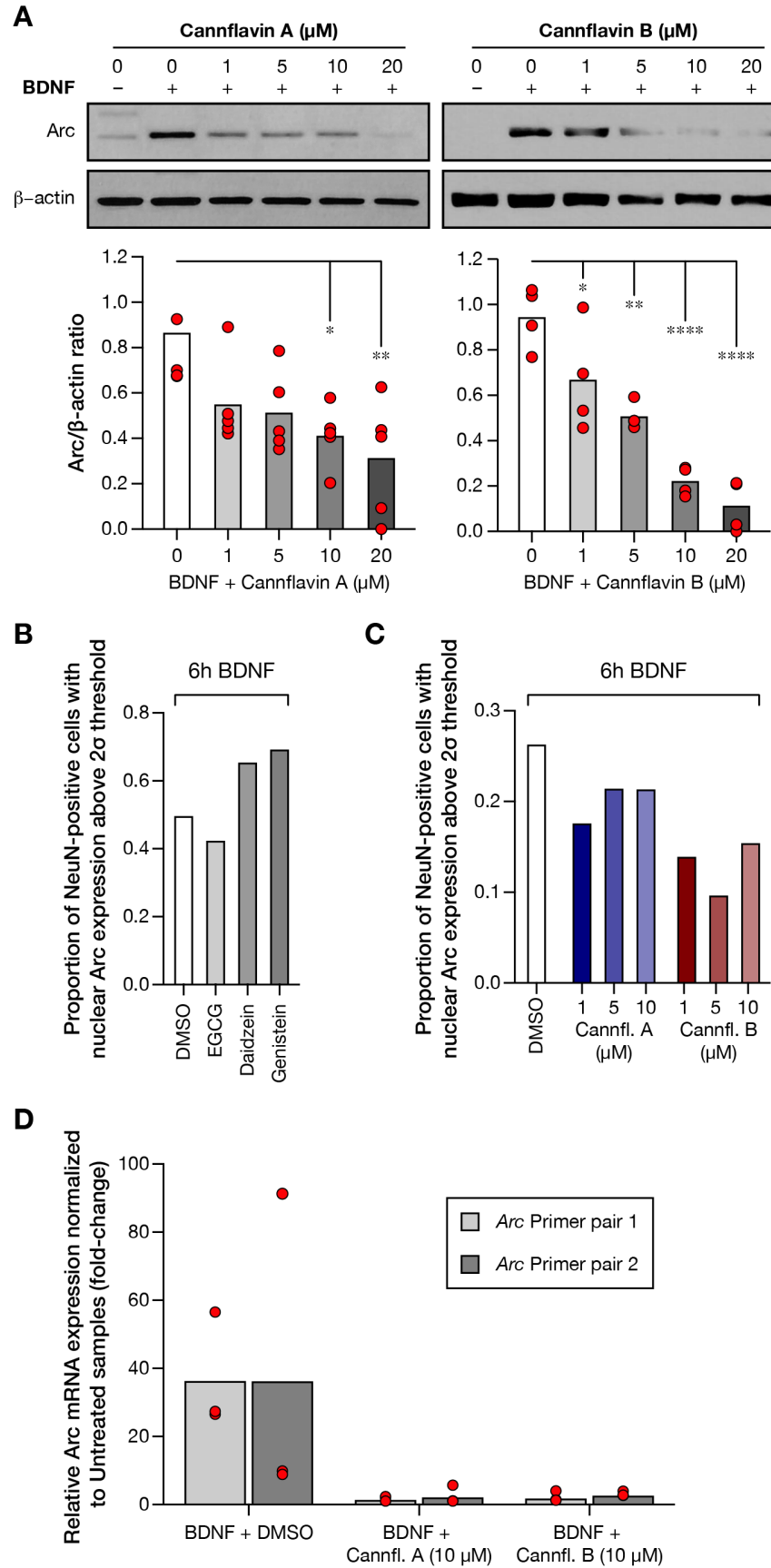
643 **Figure 1. Chemical structures of key compounds. A)** Chemical structure for cannflavin A and
644 cannflavin B. **B)** Structure for the small molecule TrkB inhibitor ANA-12. **C)** Table presenting
645 flavonoids organized by name, flavonoid class, chemical structure, and impact of BDNF-induced
646 Arc expression in mouse primary cortical neurons as reported in Lalonde et al. (2017). Position of
647 each ring is labeled for 7,8-dihydroxyflavone.

648

649

FIGURE 2

HOLBORN, WALCZYK-MOORADALLY ET AL.

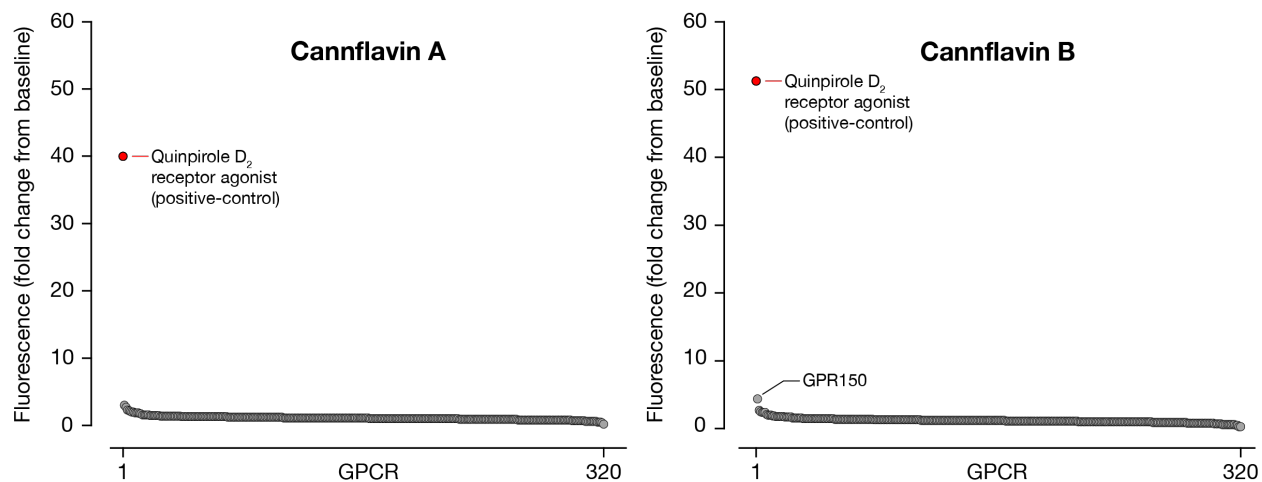


650

651 **Figure 2. Cannflavin A and cannflavin B decrease BDNF-induced Arc protein and mRNA**
652 **levels in mouse primary cortical neurons. A)** Western blot and corresponding densitometry
653 analysis showing Arc protein abundance in mouse primary cortical cultures when treated with
654 BDNF and various concentrations (0, 1, 5, 10, 20 μ M) of cannflavin A (left) or cannflavin B
655 (right). β -actin was used a loading control and graphs show mean of Arc/ β -actin ratio for each
656 condition. Biological replicates: $n = 5$ (cannflavin A), $n = 4$ (cannflavin B). One way ANOVA
657 revealed a significant decrease in the abundance of Arc with increasing cannflavin concentrations.
658 Cannflavin A ($F_{4,20} = 4.568$, $p = 0.0088$), Tukey's post-hoc test, * $p < 0.05$, ** $p < 0.001$.
659 Cannflavin B ($F_{4,15} = 24.07$, $p < 0.0001$), Tukey's post-hoc test, * $p < 0.05$, ** $p < 0.001$, **** p
660 < 0.0001 . **B)** Quantification of immunocytochemistry coverslips treated with various flavonoids
661 (EGCG, daidzein, and genistein; all 10 μ M final concentration). Quantification was completed by
662 using a ratio of Map2-positive cells with nuclear Arc above the 2σ nuclear Arc pixel intensity in
663 the control condition (BDNF treatment alone). **C)** Quantification of immunocytochemistry
664 coverslips treated with various concentrations (0, 1, 5, 10 μ M) of cannflavin A (blue bars) or
665 cannflavin B (red bars). Quantification was completed similar to B. **D)** Quantitative real-time PCR
666 *Arc* mRNA analysis using two Arc primer pairs shows a decrease in *Arc* transcripts when treated
667 with 10 μ M of cannflavin A or cannflavin B, relative to cells treated with BDNF alone.

FIGURE 3

HOLBORN, WALCZYK-MOORADALLY ET AL.



668
669

670 **Figure 3. Cannflavins do not stimulate G protein-coupled receptors signaling.** Data for 320

671 GPCRs are presented as an average fold change from baseline upon compound addition.

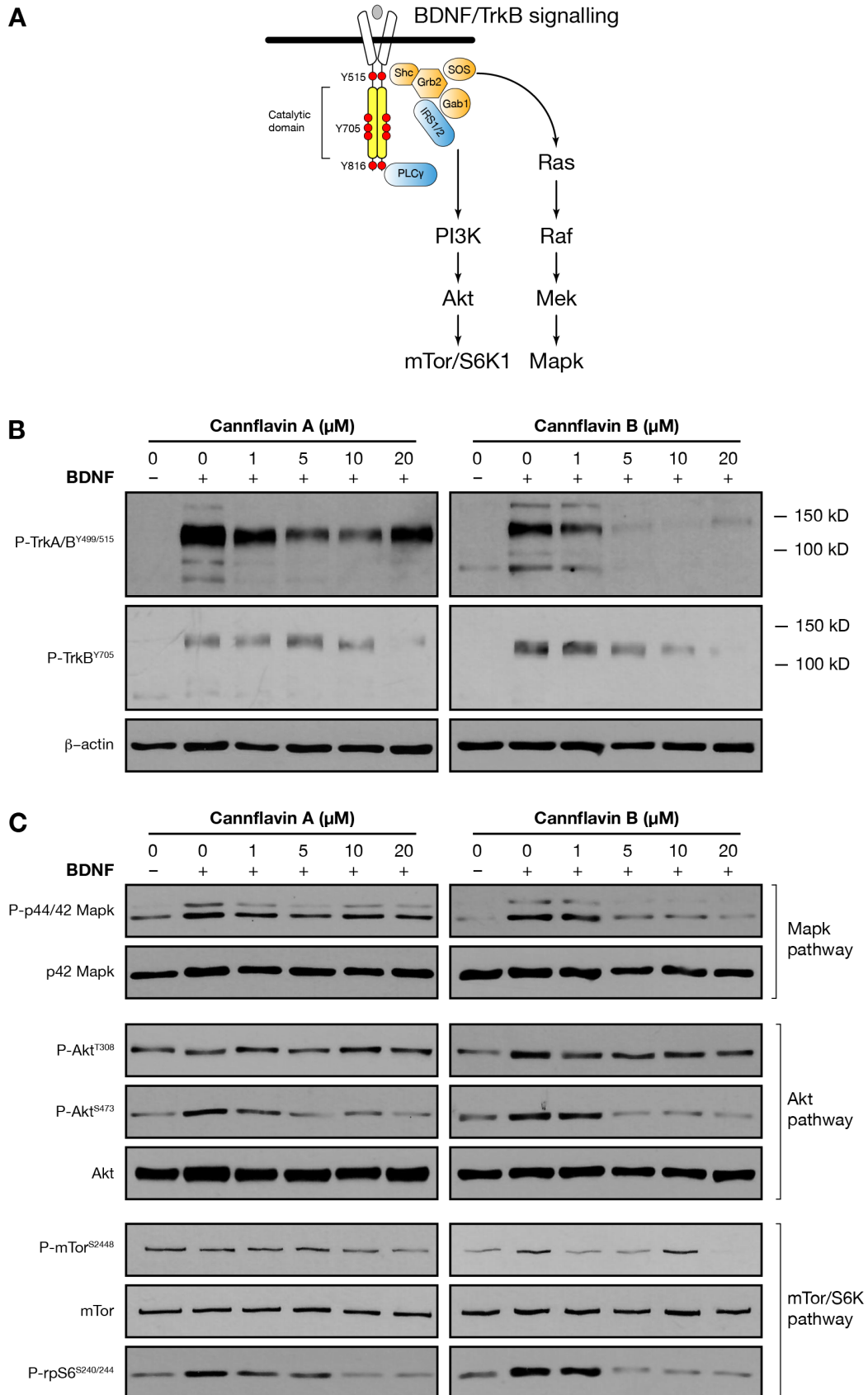
672 Application of quinpirole to D₂ receptor is used as positive control in each plate. Compounds were

673 used at 10 μ M and all tests run in quadruplicate.

FIGURE 4

HOLBORN, WALCZYK-MOORADALLY ET AL.

674



675

676

677 **Figure 4. Cannflavins A and B decrease activation of downstream pathways of TrkB. A)**

678 Simplified schematic of BDNF activation of TrkB receptors and downstream signaling pathways.

679 **B)** Western blot analysis showing phosphorylation of TrkB when treated with BDNF and various

680 concentrations (0, 1, 5, 10, 20 μ M) of cannflavin A (left) or cannflavin B (right). β -actin was used

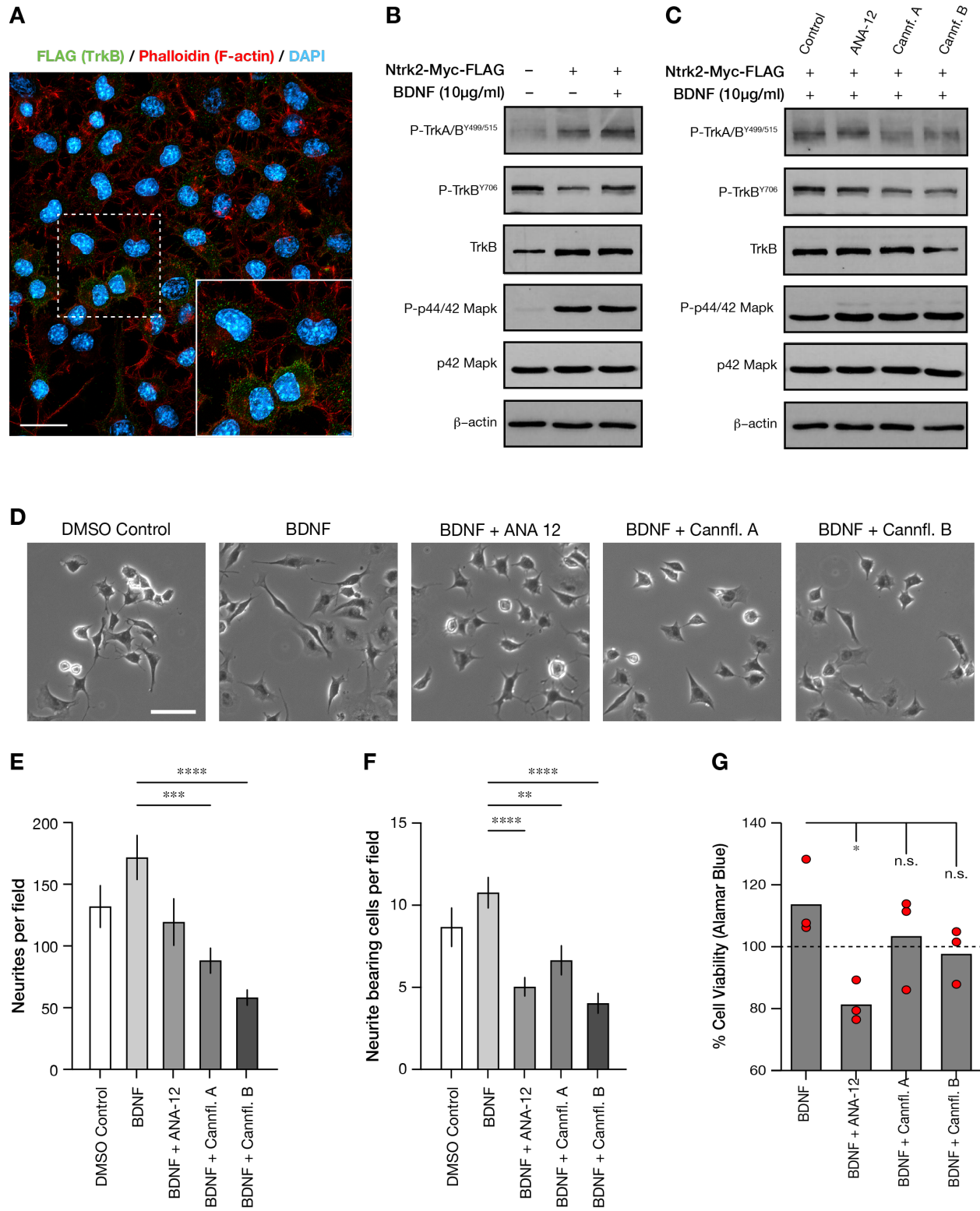
681 a loading control. **C)** Western blot analysis showing phosphorylation of Mapk, Akt, and mTor

682 proteins when treated with various concentrations (0, 1, 5, 10, 20 μ M) of cannflavin A (left) or

683 cannflavin B (right).

FIGURE 5

HOLBORN, WALCZYK-MOORADALLY ET AL.

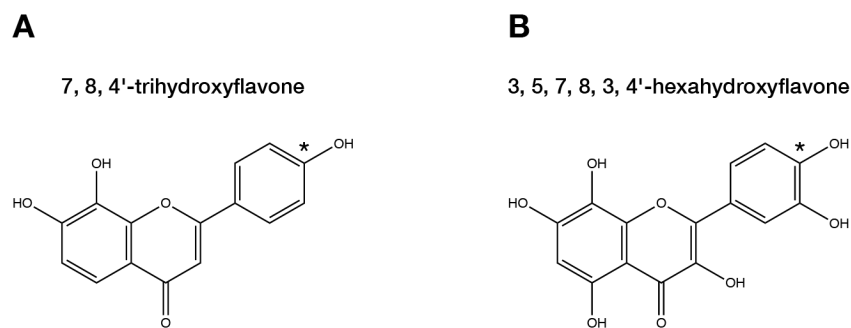


684
685
686

687 **Figure 5. Cannflavin A and cannflavin B reduces BDNF-induced neurite outgrowths in**
688 **neuroblastoma cells. A)** Neuro2a cells were transfected to stably express Ntrk2-Myc-FLAG.
689 Immunocytochemistry was completed to validate that the cells were successfully transfected. Scale
690 bar = 20 μ M. **B)** Western blot analysis showing phosphorylation of TrkB and Mapk in regular
691 Neuro2a cells compared to those stably expressing Ntrk2-Myc-FLAG. β -actin was used a loading
692 control. **C)** Western blot analysis showing phosphorylation of TrkB and Mapk when treated with
693 10 μ M of ANA-12, cannflavin A, or cannflavin B with the addition of BDNF (10 μ g/mL). The
694 small-molecule non-competitive TrkB antagonist ANA-12 was used as a positive control (Cazorla
695 et al., 2011) and β -actin was used as a loading control. **D)** Phase contrast images of Ntrk2-Myc-
696 FLAG Neuro2as treated with or without BDNF (10 μ g/mL) and 10 μ M of ANA-12, cannflavin A,
697 or cannflavin B. Scale bar = 50 μ m. Images were quantified by counting **E)** total number of
698 neurites, and **F)** total number of cells bearing neurites twice the length of cell body. One-way
699 ANOVA was used to analyze data. Total number of neurites ($F_{4,150} = 8.264$, $p < 0.001$); total
700 number of cells bearing neurites ($F_{4,150} = 9.433$, $p < 0.001$); Dunnett's multiple comparisons test
701 to BDNF condition, * $p < 0.05$; ** $p < 0.01$; *** $p < 0.001$; **** $p < 0.0001$. Graphs represent mean
702 \pm SEM. **G)** Cell viability was measured using an Alamar Blue reaction after 24 hours of treatment
703 (BDNF + ANA-12, cannflavin A, or cannflavin B). Application of ANA-12 produced a significant
704 decrease in cell viability compared to DMSO control but not cannflavin A or cannflavin B. One-
705 way ANOVA was used to analyze data. Cell survival main effect ($F_{4,10} = 3.991$, $p = 0.0345$).
706 Tukey's multiple comparisons test, * $p < 0.05$. Of note, comparison between DMSO and ANA-
707 12, specifically, was not significant ($p = 0.2532$). Graphs represent mean (3 biological replicates)
708 and dash line DMSO reference measure.

FIGURE 6

HOLBORN, WALCZYK-MOORADALLY ET AL.



709
710

711 **Figure 6.** Chemical structure of 7,8-dihydroxyflavone derivatives reported to block TrkB signaling
712 in Liu and colleagues (2010). Asterisk indicates hydroxylated 4' position on B ring of each
713 compound.

714 SUPPLEMENTARY INFORMATION FOR

715

716

717 **Interference of Neuronal TrkB Signaling by the Cannabis-Derived Flavonoids**
718 **Cannflavins A and B**

719

720 Jennifer Holborn^{1*}, Alicyia Walczyk-Mooradally^{1*}, Colby Perrin¹, Begüm Alural¹, Cara
721 Aitchison¹, Adina Borenstein¹, Jibrán Y. Khokar², Tariq A. Akhtar¹, Jasmin Lalonde¹

722

¹ Department of Molecular and Cellular Biology, University of Guelph, 50 Stone Road E,
Guelph, ON N1G 2W1, Canada.

² Department of Biomedical Science, University of Guelph, 50 Stone Road E, Guelph,
ON N1G 2W1, Canada

* J.H. and A.W.M. contributed equally to this report.

723

724 Correspondence to: Jasmin Lalonde

725

726 **Supplementary Figure 1.** Enzymatic production of cannflavin A and cannflavin B.

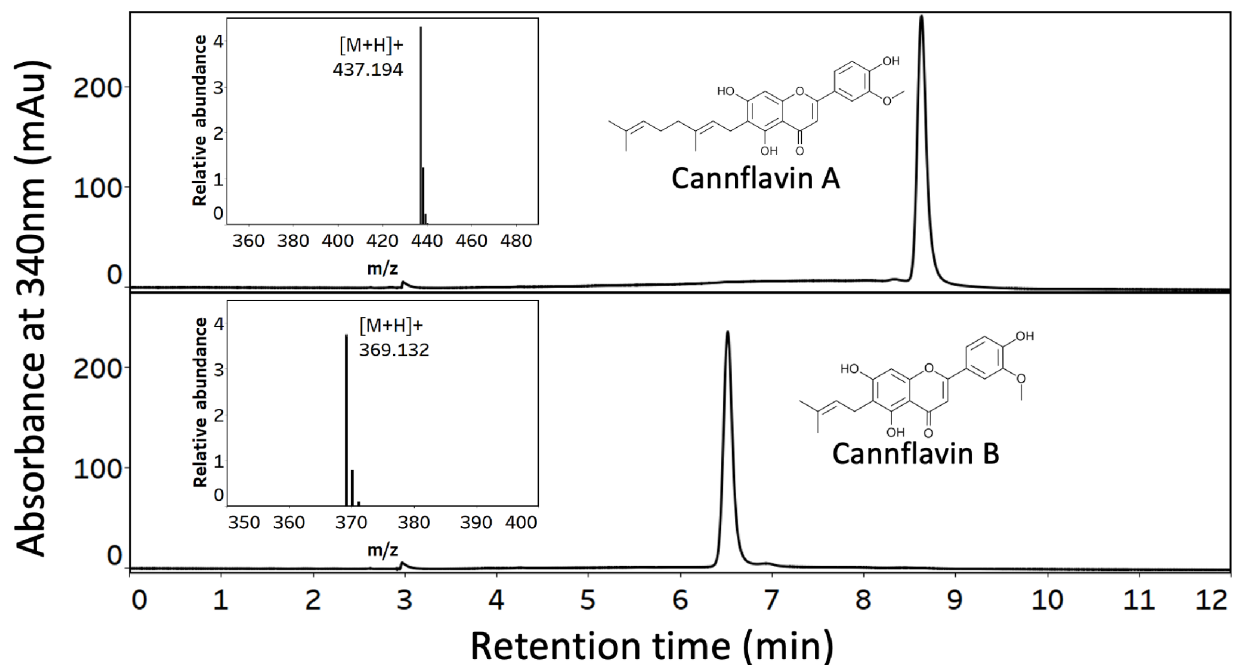
727 **Supplementary Figure 2.** Supplementary Figure 2. Effect of other flavonoids on BDNF-
728 induced Arc expression level in mouse primary cortical neurons.

729

730 **Supplementary Figure 3.** Stable overexpression of Myc-FLAG tagged TrkB increases
731 neurite outgrowths and survival in Neuro2a cells.

732

733 **Supplementary Table.** GPCRome cannflavins report.



734
735

736 **Supplementary Figure 1. Enzymatic production of cannflavin A and cannflavin B.**

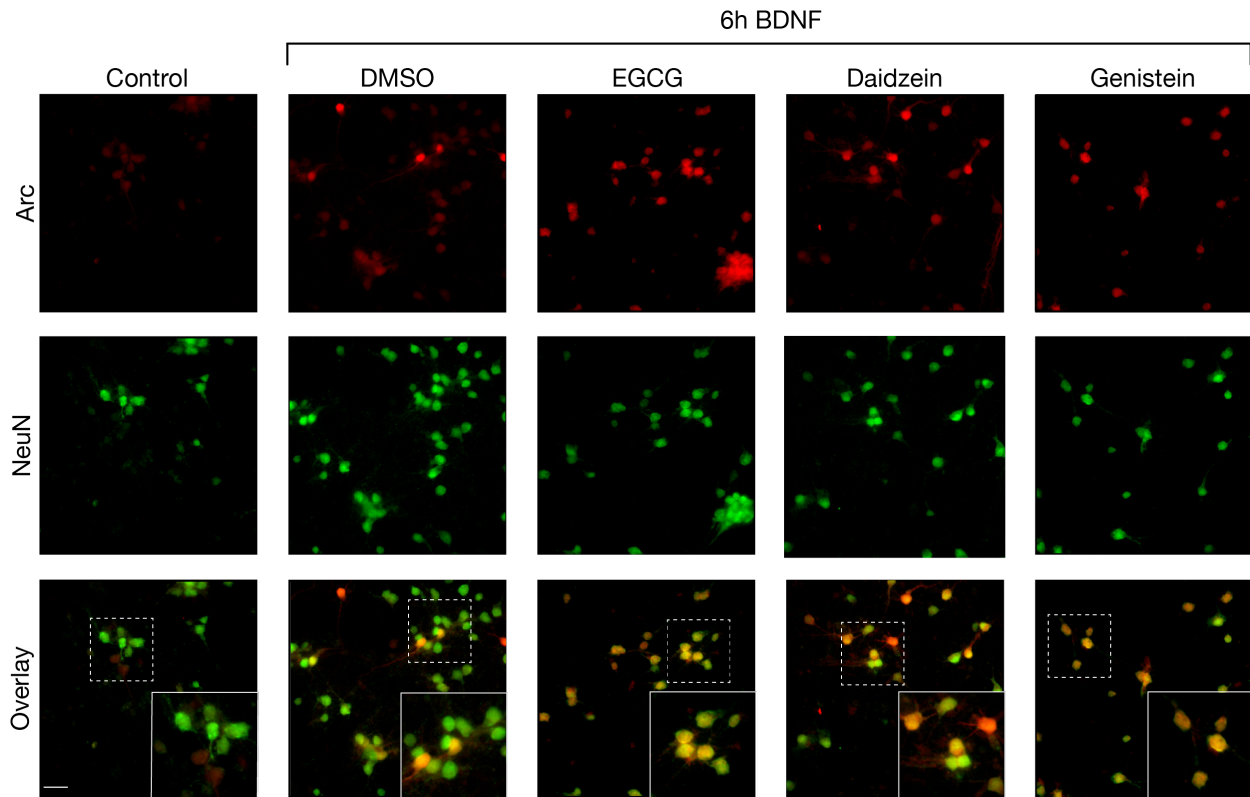
737 Representative chromatograms illustrating pooled fractions of cannflavin A (top) and cannflavin

738 B (bottom) quantified by DAD at 340 nm. Both Q-TOF mass spectra (inset) are consistent with

739 the expected m/z of 6-geranyl chrysoeriol and 6-dimethylallyl chrysoeriol or cannflavins A and B,

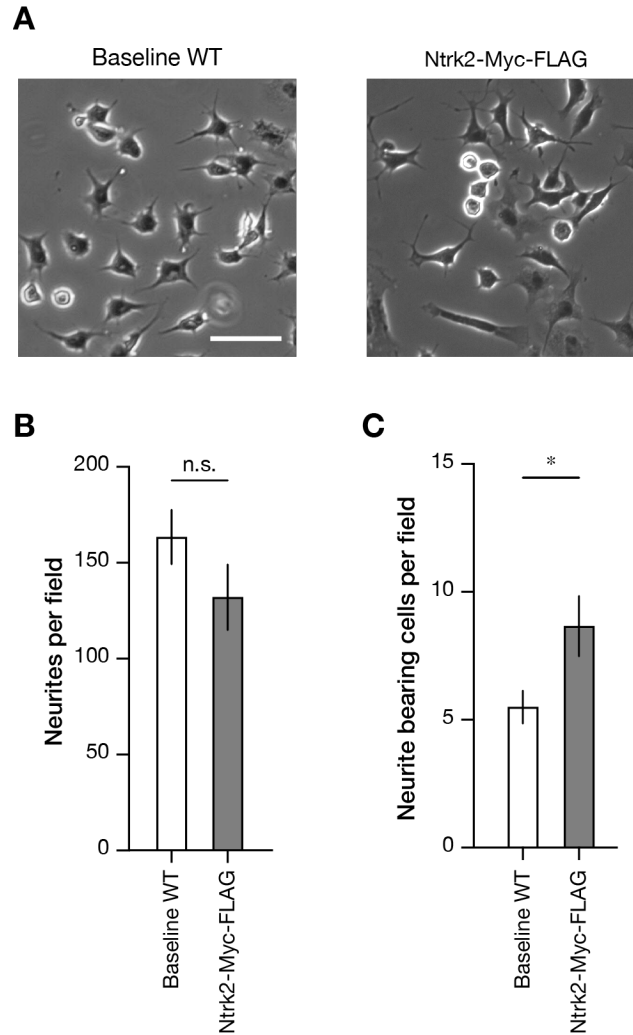
740 respectively.

741



742
743

744 **Supplementary Figure 2. Effect of other flavonoids on BDNF-induced Arc expression level**
745 **in mouse primary cortical neurons.** DIV14 cortical neurons were treated with BDNF for 6 h
746 along with EGCG, daidzein, or genistein (final concentration 10 μ M). DMSO was used as control.
747 Representative immunostaining of Arc (red fluorophore) in untreated primary cortical neurons and
748 cells that were treated with BDNF and other compounds for 6 h. Consistent with data reported in
749 Lalonde and colleagues (2017), daidzein and genistein increased Arc abundance at the tested
750 concentration. Cells were co-immunostained with the neuronal marker NeuN (green fluorophore)
751 to confirm specificity of staining to neurons. The high-magnification bottom-right insets in each
752 panel show that Arc immunostaining in a BDNF-treated culture is particularly abundant in the
753 nuclear compartment at the 6 h time point. Scale bar = 50 μ M.



754

755

756 **Supplementary Figure 3. Stable overexpression of Myc-FLAG tagged TrkB increases**

757 **neurite outgrowths and survival in Neuro2a cells. A)** Phase contrast images of wild-type (WT,

758 left) and stably overexpressing Ntrk2-Myc-FLAG (right) Neuro2a cells. Images were quantified

759 by counting **B)** total number of neurites, **C)** total number of cells bearing neurites twice the length

760 of cell body, and **D)** number of viable cells per imaged area. * $p < 0.05$, two-tailed unpaired t -test.

761 Graphs represent mean \pm SEM.

- 762 **Supplementary Table. GPCRome cannflavins report.** List of all 320 GPCRs tested in the
763 PRESTO-Tango assay.